Ionization energy of ^{6,7}Li determined by triple-resonance laser spectroscopy

B. A. Bushaw*
Chemical Sciences Division, Pacific Northwest National Laboratory, Richland, Washington 99352, USA

W. Nörtershäuser
Gesellschaft für Schwerionenforschung, 64291 Darmstadt, Germany and University of Mainz, 55128 Mainz, Germany

G. W. F. Drake
University of Windsor, Windsor, Ontario N9B 3P4, Canada

H.-J. Kluge
Gesellschaft für Schwerionenforschung, 64291 Darmstadt, Germany and University of Heidelberg, 69120 Heidelberg, Germany

(Received 6 February 2007; published 8 May 2007)

Rydberg level energies for ^{7}Li were measured using triple-resonance laser excitation, followed by drifted field ionization. In addition to the principal $n\,^2P$ series, weak Stark mixing from residual electric fields allowed observation of $n\,^2S$ and hydrogenic Stark manifold series at higher n. Limit analyses for the series yield the spectroscopic ionization energy $E_I(^7\mathrm{Li})=43\,487.159\,40(18)$ cm^{-1}. The ^{6,7}Li isotope shift (IS) was measured in selected $n\,^2P$ Rydberg levels and extrapolation to the series limit yields $\mathrm{IS}(E_I)^{7,6}=18\,067.54(21)$ MHz. Results are compared with recent theoretical calculations: E_I values from experiment and theory agree to within 0.0011 cm^{-1}, with the remaining discrepancy comparable to uncertainty in QED corrections of order $\alpha^4 Ry$. The difference between experiment and calculated mass-based $\mathrm{IS}(E_I)$ yields a change in nuclear charge radii between the two isotopes $\delta\langle r^2\rangle^{7,6}=-0.60(10)$ fm^2.

DOI: 10.1103/PhysRevA.75.052503 PACS number(s): 32.10.Hq, 32.80.Rm, 42.62.Fi

I. INTRODUCTION

Precise measurement of the lithium ionization energy is important for testing recent advances in calculations on few-particle systems [1–3]. In addition to their intrinsic interest, these calculations are an essential underpinning for optical measurements that investigate changes in nuclear charge distribution for the short-lived radioisotopes ^{8,9,11}Li [4,5]. These measurements focus on how the two halo neutrons of ^{11}Li affect the charge distribution of the ^{9}Li-like nuclear core, a subject of considerable current interest in nuclear physics [6]. Recent atomic physics calculations that include complete accounting for QED shifts up to order $\alpha^3 Ry$ have yielded refined values for both the ionization energy and the $2s\,^2S$-$3s\,^2S$ transition energy of ^{7}Li with estimated accuracy better than 0.001 cm^{-1} [7]. Results for both are in good agreement with existing experimental data, but theoretical uncertainties are now smaller than experimental. Thus, improved experimental values are desirable for further refining and testing of theory, and consequently insuring that mass and nuclear volume effects can be accurately separated in the online radioisotope studies.

Recent measurement of the $2\,^2S$-$3\,^2S$ energy [8] decreased experimental uncertainty about 10-fold over previous discharge lamp Fourier transform measurements [9] and showed a closer agreement (+0.0016 cm^{-1}) with the calculated value. The $2\,^2S$-$3\,^2S$ energy in Ref. [8] has been independently confirmed by beat frequency methods referenced to an I_2 hyperfine stabilized diode laser [10].

The accepted value for the ^{7}Li ionization energy of 43 487.150(5) cm^{-1} [11] is derived from classic atomic emission measurements [12] that were combined with newer measurements and reanalyzed by Johannson in 1959 [13], with the resulting value "thought to be correct within 0.005 cm^{-1}." However, remeasurement of a few transitions with laser-wavemeter methods suggested uncertainty more on the order of 0.030 cm^{-1} [14]. More recently, pulsed laser studies have examined the $nf\,^2F$ [15], and $np\,^2P$ [16] Rydberg series, but precision in the derived E_I values do not seem to improve on the accepted value. The most recent theoretical value $E_I(^7\mathrm{Li})=43\,487.1583(6)$ cm^{-1} [7] is in reasonable agreement with the accepted value, but has estimated precision that is better by more than an order of magnitude.

Most of the alkali metals have had their ionization energies precisely determined by Rydberg series spectroscopy [14,17–20], but studies on Li are lacking because of interference from one-photon absorption by Li_2 dimers in the same 460–470 nm region as the two-photon-excited atomic Rydberg series [21,22]. We use stepwise excitation with three (red) high-resolution single-mode lasers, followed by drifted rf-field ionization and mass analysis, to detect the Rydberg series. In this work, Rydberg structure observed out to $n\approx 300$ is dominated by the principal $np\,^2P$ series, but weak residual electric fields also allow observation of the $ns\,^2S$ series and series of hydrogenic Stark manifolds (HSM) at higher n. For determination of the ionization energy, convergence analyses on the predominant $np\,^2P$ series ($n=28$ to 175) yields the value $E_I(^7\mathrm{Li})=43\,487.159\,40(18)$ cm^{-1}, while the other series and measurements at higher electric field confirm the value, as well as the correction used for residual Stark shifts. Uncertainty in the relative series con-

*Electronic address: bruce.bushaw@pnl.gov

vergence limit is lower, on the order of 10^{-5} cm^{-1}; the major source of uncertainty in the final value is in the absolute energies of the transitions linking a reference Rydberg level to the ground state. In addition to $E_I(^7\mathrm{Li})$, ^{7}Li-^{6}Li isotope shifts were measured for a number of high-lying Rydberg levels and extrapolation to the series limit yields the isotope shift of E_I with precision at the 200 kHz level. These results are compared to theoretical calculations.

II. EXPERIMENT

The experimental apparatus and general methodology have been described in previous papers [23,24] and are only briefly summarized here. Within a field-free interaction region, ^{7}Li in a collimated atomic beam ($\approx$1 mrad, natural isotopic abundances) is excited to high-lying Rydberg levels by three single-mode cw lasers (diode, Ti-sapphire, dye) via

$$2s\ ^2S_{1/2}(F=2) \xrightarrow{671\ \mathrm{nm}} 2p\ ^2P_{1/2}(F=2) \xrightarrow{813\ \mathrm{nm}} 3s\ ^2S_{1/2}(F=2) \xrightarrow{\approx 614\ \mathrm{nm}} np\ ^2P. \quad (1)$$

The long-lived Rydberg atoms then drift out of the interaction region into a quadrupole mass filter (QMF) where they are ionized by rf fields. Continued passage through the QMF provides mass selection and transmitted ions are detected with an off-axis continuous dynode multiplier. Similar excitation schemes have been used for selective analytical measurements [25] and for measuring hyperfine structure (hfs) in the 3 ^2S level using Stark spectroscopy [26], but neither reported Rydberg level energies.

Relative laser frequencies are controlled by interferometric offset locking to a stabilized single-frequency He:Ne laser [27] with a confocal Fabry-Perot interferometer [CFI, free spectral range (FSR)=148.629 65(6) MHz] and are known with an accuracy of $\approx 5\times10^{-5}$ cm^{-1} (1.5 MHz) over the $\approx$120 cm^{-1} range below E_I studied here. Absolute laser frequencies are determined with an accuracy of $\approx$2 MHz using a carefully aligned wavemeter that is calibrated against known frequency standards. Relevant calibrations used for these experiments are the ^{7}Li 2 $^2S_{1/2}$-2 $^2P_{1/2}(F=1\rightarrow2)$ transition at 671 nm [28], the ^{40}Ca 657-nm $4s^2\ ^1S_0$-$4s4p\ ^3P_1$ intercombination line [29,30], the ^{85}Rb 5 $^2S_{1/2}$-5 $^2D_{5/2}(F=3\rightarrow5)$ two-photon transition at 778 nm [31], and the ^{133}Cs $D_2(F=4\rightarrow5)$ transition at 852 nm [32]. After calibration on the 852 nm Cs line, our determinations for the other three wavelengths agree with the accepted values to within 1.7 MHz (average: −0.76 MHz from reference values).

Because of large Doppler shifts for lithium, atomic beam–laser beam perpendicularity is critical for accurate measurement of absolute energies. This was tested and adjusted with $1+1'$ ionization: the 671 nm resonance laser populated the $2P$ levels, which were then directly photoionized with the 345 nm line from an argon ion laser. The 671 nm beam was retroreflected and carefully aligned through translatable apertures separated by 1.2 m on either side of the atomic beam.

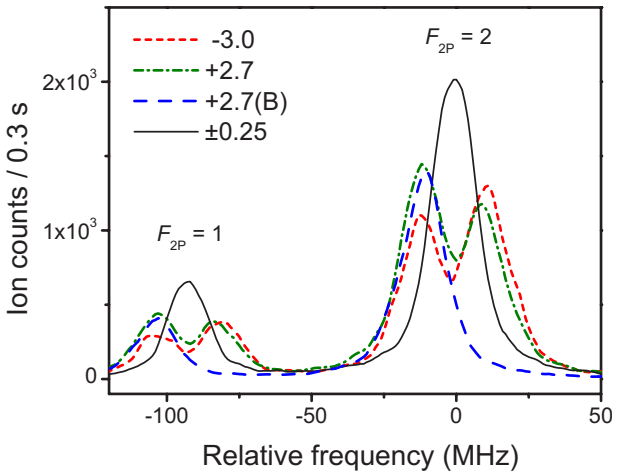

FIG. 1. (Color online) Setting atomic beam–laser beam perpendicularity. Excitation of ^{7}Li 2 $^2S_{1/2}(F=2)\rightarrow2\ ^2P_{1/2}$ with retroreflected 671 nm laser; ionization with 345 nm argon ion laser. Deviations from perpendicularity of input beam in mrad, (B) retroreflected beam blocked.

If there is significant deviation from perpendicularity between laser and atomic beams, the result is a bimodal peak (Fig. 1) corresponding to equal but opposite Doppler-shifted distributions for the two directions. The difference in intensity between the peaks is caused by four additional Fresnel reflection losses experienced by the retroreflected beam exiting and reentering through the vacuum chamber window. Changing the intersection angle by countermoving the apertures and realigning allows determination of the crossing point for the two Doppler-shifted peaks, corresponding to true perpendicularity. From the 0.25 mrad uncertainty in the crossing point, the corresponding residual Doppler shift uncertainty is $\approx$1 MHz.

For triple-resonance excitation to Rydberg levels, the 813 nm and 614 nm lasers are carefully overlapped with the aligned 671 nm laser (angular deviation $<$0.1 mrad), and with counterpropagation of successive excitation steps. Frequencies of the first two lasers are centered by tuning the third step slightly above the ionization limit ($\approx$611 nm) and observing direct photoionization. While centering of the individual steps is within 3 MHz, the sum frequency can be set with an accuracy of $\approx$0.5 MHz to selectively populate the $3s\ ^2S_{1/2}(F=2)$ intermediate excited state. The third step laser is then tuned near a high Rydberg level ($n\approx150$), and electric fields within the interaction region are minimized by adjusting correction electrodes in three dimensions to minimize the Stark redshift in the observed resonance position [24].

The overall approach is to carefully measure the energy of a reference Rydberg level (we use $n=76$) and then use relative frequencies to calculate the energies of other levels. For high n ($>$70), where levels are closely spaced, resonances were observed using continuous scanning with fringe-offset-locking, as previously described in Ref. [23]. Transitions could also be investigated in individual short scans that were still linked to the reference level by fringe-offset-locking, using the wavemeter to confirm CFI order number, as shown in Fig. 2.

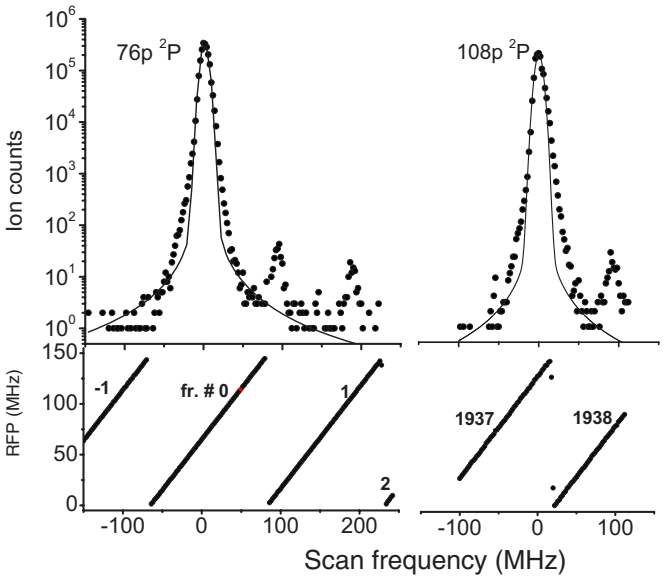

FIG. 2. Determination of relative Rydberg level energies. Upper: ionization signal in high resolution scans; weak peaks are from off-resonance excitation of unselected hyperfine levels in the first two transitions. Lower traces are the relative fringe position (RFP), within the indicated CFI order [FSR =148.629 65(6) MHz], measured with respect to a fixed fringe of the reference He:Ne laser.

For determination of the reference level absolute energy, the energy of the third-step laser was added to the known energy of the 3 ^2S second excited level [8,10]. With several measurement sets over the course of these experiments, we find the ^{7}Li 3 $^2S(F=2)$-76 ^2P transition energy to be 16 262.04 190(7) cm^{-1}, and the corresponding energy of 76 ^2P above the center of gravity (c.g.) of the ground level hyperfine structure is 43 468.138 43(17) cm^{-1}.

III. RESULTS AND DISCUSSION

A. Rydberg spectra

Figure 3 shows the Rydberg spectrum observed for ^{7}Li

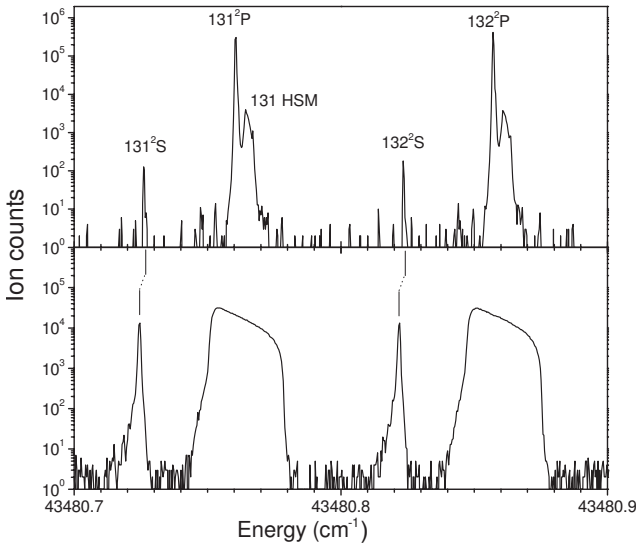

FIG. 4. Detailed structure observed in the Rydberg spectra of ^{7}Li near $n=131$ obtained by triple-resonance excitation. Upper section shows minimized electric field ($\lesssim$0.3 mV/cm), lower section shows field $\approx$20 mV/cm. HSM denotes hydrogenic Stark manifold.

over the last $\approx$20 cm^{-1} below E_I, obtained with minimized electric field. Below $n\approx 80$, only members of the np ^2P series are observed, and with better than five orders of signal to background. A weak substructure grows at higher n, as shown in the vicinity of $n=131-132$ in Fig. 4. In the minimized field case ($\approx$0.3 mV/cm) the n ^2P series is the dominant feature and is still well resolved, but because of Stark mixing from the residual field, the ^2S series appears weakly (3×10^{-4} relative intensity) at quantum defect $\delta_S\approx 0.4$. Broader peaks appear at energies slightly higher than the ^2P levels (centered around $\delta=0$), and are attributed to manifolds of Stark states, corresponding to the zero-field $\ell=2$ to $n-1$ higher orbital angular momentum states. The effect of increased electric field ($\approx$20 mV/cm) is shown in the bottom of Fig. 4: the Stark manifold broadens and subsumes the ^2P levels as the manifold width becomes $>2\delta_P$; while the ^2S

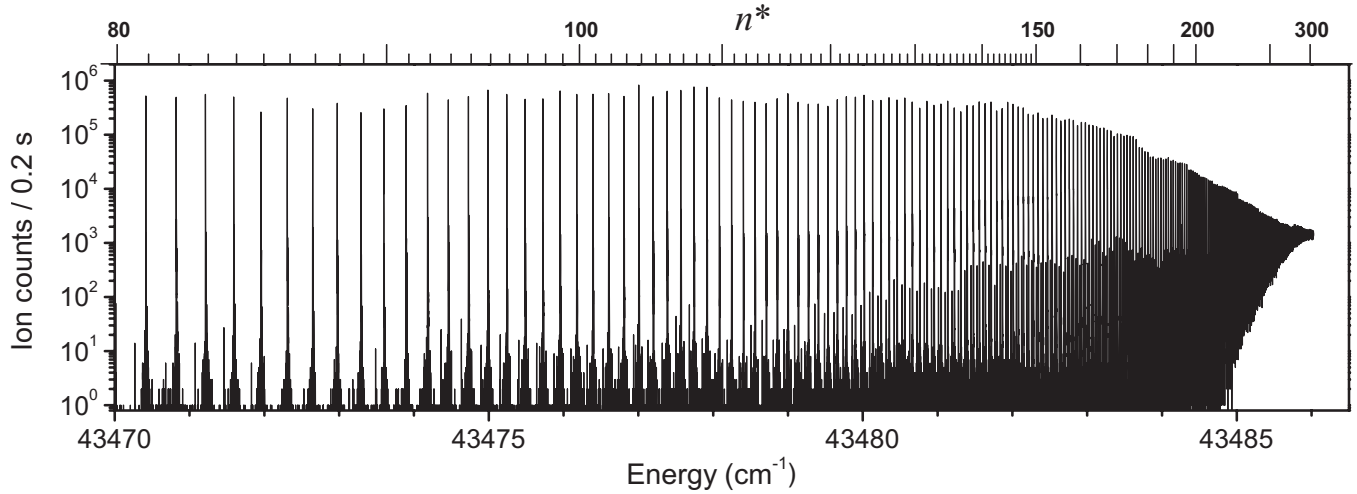

FIG. 3. Rydberg spectrum of ^{7}Li obtained by triple-resonance excitation and drifted field ionization, minimized electric field in the excitation region. Principal structure is the n ^2P series. Unresolved weak structure above $n\approx 100$ are detailed in Fig. 4.

TABLE I. Ionization energy and limit quantum defects determined from convergence analysis on Rydberg series of ^{7}Li. Uncertainties in parentheses include only the statistical uncertainty (1σ) from the fitting procedure.

Set	Series	n range	Field[a]	E_I (cm^{-1})	E_I (cm^{-1}) (n.s.)[b]	δ_0
1	$np\ ^2P$	70–170	min	43487.15931(2)	43487.15915(2)	0.04709(5)
2	$ns\ ^2S$	93–178	min	43487.15945(2)	43487.15929(1)	0.39977(13)
3	$ns\ ^2S$	83–144	20	43487.15917(9)	43487.15856(6)	0.39744(32)
4	$np\ ^2P$	76–110	20	43487.1594(9)	43487.1558(10)	0.051(7)
5	HSM	76–164	20	43487.15932(5)		$\equiv 0$
6	$np\ ^2P$	28–93	min	43487.159347(11)		0.047180(11)
7	$np\ ^2P$	28–153	min	43487.159416(6)	43487.159400(4)	0.047230(7)
8	$np\ ^2P$[c]	28–175	min	43487.159395(3)	43487.159287(9)	0.047192(5)

[a]$20 \approx$ mV/cm estimated from Simion field calculations and applied correction potential. min: ≈ 3 mV/cm estimated by comparing fit Stark coefficient with higher field case.
[b]No Stark correction.
[c]Fit level energies average of three to eight measurements on different days.

levels remain distinct, become much stronger, and are only slightly shifted. This structure is completely analogous to the $n=15$ behavior examined in the seminal work of Kleppner *et al.* [33]; however, our electric field is in the mV/cm range instead of kV/cm, and we do not resolve the (many more) individual Stark states. For determination of the ionization energy, it is important to note that, as long as the electric field perturbations are small, the induced shifts in the ^2S and ^2P series scale proportional to $F^2(n^*)^7$ [34].

For $n>70$, Rydberg spectra were recorded as continuous scans (Fig. 3), both with minimized and ≈ 20 mV/cm electric fields. More detailed investigation examined the ^2P series for $n=28-175$ at minimized field using both continuous and localized, higher resolution scans (Fig. 2). Observed peaks were fit with Voigt profiles (statistical weighting) while positions within the CFI order were obtained by linear fitting of the simultaneously recorded CFI fringe position (bottom of Fig. 2). Typical statistical uncertainty for fitting peak centroids was ≈ 200 kHz, and average standard deviation for repeated measurements taken on different days was 600 kHz (2×10^{-5} cm^{-1}). We do not tabulate values for all of the individual levels here, but note that they are all reproduced within 6×10^{-5} cm^{-1} by the simple Rydberg-Ritz formula discussed below.

B. ^{7}Li ionization energy

The energies of levels within a given Rydberg series for a one-valence-electron atom can be described by the Rydberg-Ritz equation:

$$E_n = E_I - \frac{R_M}{(n^*)^2}, \tag{2}$$

where R_M is the mass-reduced Rydberg constant for the particular isotope; $R(^7\mathrm{Li})=109\,728.735\,348$ cm^{-1}, based on CODATA 2002 values for R_∞ and electron mass [35], and ^{7}Li mass from AME 2003 [36]. A new determination of the ^{7}Li mass [37] has yielded a value $1.1\times10^{-6}u$ lower than the AME 2003 value, but this does not alter our results at the current level of precision. The effective principal quantum number n^* is expressed in terms of a state specific quantum defect, where the variation with n is generally expanded in inverse even powers of n^*,

$$\delta_n = \delta_0 + \frac{a_1}{(n^*)^2} + \frac{a_2}{(n^*)^4} + \cdots \tag{3}$$

to account for small, slowly varying changes in quantum defect at low n, which may be caused by core polarization, relativistic effects, and incomplete wave-function recapitulation. The formulation (3), generally requires an iterative solution, but, because of the compact $1s^2$ core of lithium and because we study higher levels ($n \geqslant 28$), only the first expansion term is needed (indeed, for data sets with $n>70$, the original Rydberg formula with constant quantum defect is sufficient). Also, the constant approximation $n^*=n-\delta_0$ has been used for calculation of the Ritz terms [19]; this may cause small shifts in determined Ritz coefficients a_n, but has negligible effect on either E_I or the limit quantum defect δ_0. Thus the measured level energies are fit according to

$$E_n = E_I - \frac{R_M}{n_0^2} + c_S n_0^7, \tag{4}$$

where $n_0=n-\delta_0-a_1/(n-\delta_0)^2$, and the final term is the Stark shift correction. Fitting was done by Levenberg-Marquardt nonlinear least squares with fit parameters E_I, δ_0, a_1, and c_S. For data sets taken from a single spectrum, the measured level energies were equally weighted with $\sigma=6\times10^{-5}$ cm^{-1}, the average day-to-day reproducibility. For the data sets with multiple determinations for each level, weights were the actual standard errors. Both a_1 and c_S could be fixed at zero to examine the effect of the Stark and Ritz terms. Results from a number of measurements are summarized in Table I.

The first two data sets, for the $n\ ^2P$ and $n\ ^2S$ series, are derived from the same experimental spectrum (Fig. 2). Agreement between the two series is relatively good, within 1.4×10^{-4} cm^{-1}, but greater than the combined uncertainty.

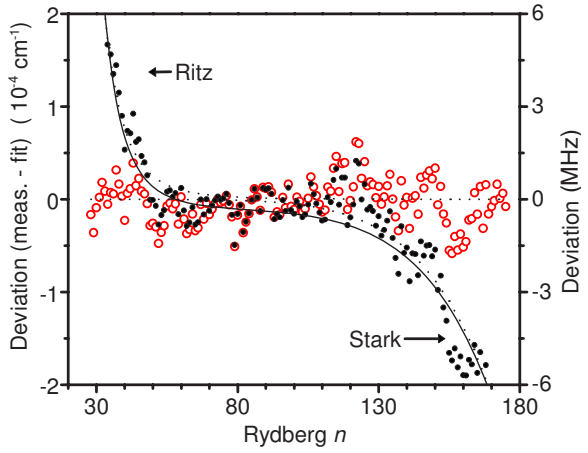

FIG. 5. (Color online) Deviations between measured and fit level energies for the ^{7}Li $n\,^2P$ Rydberg series, $n=28-175$. Open circles (red) fit with all four parameters (E_I, δ_0, a_1, and c_S) free. Solid points illustrate the effect of Ritz and Stark terms: E_I and δ_0 set at the full free-fit values, a_1 and c_S fixed at zero.

The apparent E_I values are slightly lowered if no Stark correction is applied. Including the first Ritz expansion term caused no significant change in the E_I values and uncertainty in the derived coefficient was more than 3 times its absolute value. Thus, for all high-n data sets (1–5) the Ritz term was fixed at zero.

The next three sets (3–5) were recorded similarly, but with an electric field $\approx$20 mV/cm applied along the atomic beam axis. The effect on the spectra was shown in Fig. 4. Because of the larger field effects, analysis for the $n\,^2S$ and $n\,^2P$ series was constrained to lower n, where they are well separated from the expanding HSM; thus, the precision is somewhat less. Without the Stark correction, the determined E_I values are significantly lower than with minimized field, and as expected, much more so for the $n\,^2P$ series. The Stark corrected values are brought back into good agreement with the higher precision low-field measurements, giving confidence that the smaller corrections for the minimized field case are correct. For the HSM observed in the same spectrum, centers were estimated as equidistant from the two sharp edges of the distribution (see lower trace in Fig. 4), and a simple fit with E_I as the only free variable yielded a value that is in good agreement with the $n\,^2P$ and $n\,^2S$ series.

Sets 6–8, for the $n\,^2P$ series at minimized field and starting at $n=28$, show good agreement with each other and the high-n data sets. Sets 6 and 7 were each completed in 1 day with only one determination for each n, while set 8 was obtained over a period of several weeks with multiple determinations for each n. Set 6, with maximum n of 93, could not be reliably fit with c_S as a free variable because the Stark shifts below $n=100$ are negligible. For sets 7 and 8, changes in E_I from Stark correction are small but statistically significant. Inclusion of the first Ritz term was marginally significant; if not included, the derived E_I values were $\approx 2\times10^{-5}$ cm^{-1} higher.

The quality of the fit for the full data set (8) is illustrated in Fig. 5, which shows the deviations between the measured and fit energy levels: the maximum deviation is 6.2 $\times10^{-5}$ cm^{-1} and the average is 1.9×10^{-5} cm^{-1}. The figure also illustrates the nature and magnitude of the Ritz and Stark corrections. Statistical uncertainty for the convergence limit is $\approx 3\times10^{-6}$ cm^{-1}, but analysis on subsets ($n\leqslant100$ and $n>100$), where Stark and Ritz terms, respectively, become insignificant, as well as allowing higher-order Ritz terms, indicate that real uncertainty is on the order of 3×10^{-5} cm^{-1}. This is primarily due to systematic errors from drift in the residual electric field, reflected by the fact that $\chi_r^2=1.0005$ for the low-n subset while $\chi_r^2=2.87$ for the high-n subset. Values for derived atomic parameters are given in Table II.

TABLE II. Atomic parameters determined for ^{7}Li.

Parameter	This work	Microwave[a]
E_I (cm^{-1})	43487.159395(33)	
$\delta_0(n\,^2S)$	0.3994(7)	0.399510(1)
$\delta_0(n\,^2P)$	0.04720(2)	0.047170(2)
$\delta_1(n\,^2P)$	−0.040(13)	−0.024(1)

[a]From Ref. [38], $\delta_0(n\,^2P)$ is an intensity weighted average for $n\,^2P_{1/2}$ and $n\,^2P_{3/2}$ values of 0.047 178 0(20) and 0.047 166 5(20), which are not resolved in our measurements.

The uncertainty for $E_I(^7\mathrm{Li})$ in Table II is only the statistical uncertainty derived from the various data sets given in Table I; additional systematic errors for the E_I determination are discussed below. The limit quantum defects show good agreement with values determined by microwave measurement of $n-(n+1)$ level intervals [38]; however, those measurements did not yield a value for E_I. The Ritz coefficient for the $n\,^2P$ series is relatively imprecise because only $n\geqslant28$ are studied, and δ_n has already nearly converged to δ_0 ($\delta_{28}=0.047\,143$). This could be improved by adding measurements at lower n, but was not the focus of this work and might require including higher-order Ritz terms. No Ritz coefficient was determined for the $n\,^2S$ series, because it was observed only for $n>80$ and $a_1(n\,^2S)=0.029$ determined in Ref. [38] indicates that the effect is of similar magnitude (but opposite sign) as in the $n\,^2P$ series.

In addition to the statistical uncertainty for $E_I(^7\mathrm{Li})$ given in Table II, there are other possible systematic errors, which are detailed in Table III. The first two entries are determined with the same instrumental method (wavemeter) and calibrations; thus, the uncertainties may be correlated and are added

TABLE III. Sources of uncertainty in determination of the ^{7}Li ionization energy. Components and their addition are discussed in the text.

Source	Uncertainty (10^{-5} cm^{-1})
$3\,^2S_{1/2}$ energy	10
$3\,^2S$-$76\,^2P$ energy	7
Beam perpendicularity	3
Interferometer scale	2
Convergence above $76\,^2P$	3.3
Total	17.7

TABLE IV. Summary of experimental and theoretical values for bound transition energies and E_I of ^{7}Li, values in cm^{-1}.

Transition	Experiment	Reference	Theory	Reference	Δ (10^{-4} cm^{-1})
^2S-2 $^2P_{1/2}$	14903.648130(14)	[28]	14903.6478(10)	[a]	−3.3 (10)
2S-3S	27206.09420(10)	[8]	27206.0926(9)	[7]	−16 (9)
2S-E_I	43487.15940(18)	This paper	43487.15830(60)	[7]	−11 (6)

[a]14 903.647 7(39) cm^{-1} from Ref. [39], revised after comparison with Bethe logarithms in Ref. [7].

linearly. The other terms are then added in quadrature. Beam perpendicularity and interferometer scale (relative uncertainty in the CFI-FSR projected over the energy between the 76 ^2P level and the convergence limit) were discussed in the experimental section. The total uncertainty is clearly dominated by the first two entries, which define the reference level energy. From this, we obtain the final value for the experimental ^{7}Li ionization energy:

$$E_I(^7\mathrm{Li})_{\mathrm{expt}} = 43\,487.159\,40(18) \tag{5}$$

given with respect to the hfs c.g. in the 2 ^2S ground level. This may be compared with the most recent theoretical value [7],

$$E_I(^7\mathrm{Li})_{\mathrm{theo}} = 43\,487.158\,30(60). \tag{6}$$

Although the agreement is now quite good, at the 1×10^{-3} cm^{-1} level and nearly within the combined uncertainties, similar residual discrepancies are also observed for the 2 ^2S-3 ^2S and 2 ^2S-2 $^2P_{1/2}$ transitions energies, as summarized in Table IV.

The residual differences are of the same order as the uncertainty of 4×10^{-4} cm^{-1} for the higher-order QED corrections given in Ref. [7], and may give guidance to further development of these difficult to evaluate terms. Very accurate measurements of the ^{6,7}Li 2 ^2S-4 ^2S transition energies [40] may also contribute to understanding this problem, if corresponding theoretical calculations are performed.

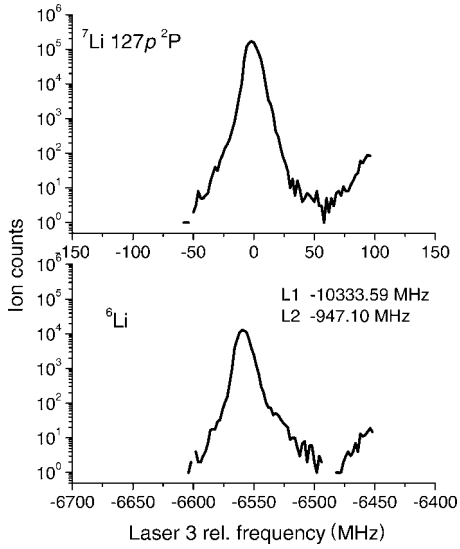

FIG. 6. Isotope shift measurement for the 127 ^2p level.

C. ^{6,7}Li isotope shift of ionization energy

While absolute energies may be the best overall test of theory, with relative accuracies for both experiment and theory approaching the 10^{-8} level, isotope shifts are also of considerable interest. Many mass-independent terms in the theory, and their associated uncertainties, cancel for isotopic shift in transition energies, and theoretical uncertainties are on the order of 15 kHz (5×10^{-7} cm^{-1}). This is an order of magnitude smaller than uncertainty arising from imprecise knowledge of the nuclear charge distributions, and is indeed the basis for optical investigation of lithium nuclear charge radii [4,5]. The experimental situation is similar: the relatively small intervals of isotope shifts are more easily measured, and generally with greater accuracy, than absolute transition energies. Hence, for measurement of the isotope shift of the ionization energy between ^{7}Li and ^{6}Li, we do not perform an independent measurement of $E_I(^6\mathrm{Li})$ as described for ^{7}Li in the preceding section, but rather measure the isotope shift in a series of Rydberg levels and extrapolate to the ionization limit. The isotope shifts in the 2 $^2P_{1/2}$ and 3 $^2S_{1/2}$ levels were examined in detail in Refs. [8,28], thus simplifying the triple-resonance measurement of IS in the Rydberg levels. After finding, centering, and recording a reference ^{7}Li spectrum for given n ^2P Rydberg level; the first and second step lasers are respectively tuned −10 333.59 and −947.10 MHz to excite ^{6}Li on the hyperfine path $F=3/2\rightarrow3/2\rightarrow3\,^2S_{1/2}(F=3/2)$, the mass spectrometer is switched to mass 6, and the third step laser is scanned over the region of the expected Rydberg resonance. An example measurement for $n=127$ is shown in Fig. 6. Similar measurements were repeated for selected, approximately equally spaced in energy, Rydberg levels over the range of $n=37-145$, with results shown in Fig. 7. The term energies (E_n-E_I) are calculated with the Rydberg formula [Eq. (2)] using R_6 and $\delta_0=0.047\,20$. Linear fitting of the measured shifts yields a slope of −0.3925(60) MHz/cm^{-1}=1.31(2)$\times10^{-5}$ (unitless), which can be compared to the normal mass shift coefficient: $M_{\mathrm{NMS}}=(u/m_e)(M_6-M_7)/M_6M_7=1.301\times10^{-5}$. It is not surprising that changes in the isotope shift between Rydberg levels is completely accounted for by the normal mass shift, i.e., any specific mass shift or nuclear field shift comes from removal of the 2s electron, not the particular Rydberg level to which it is promoted. The intercept of the same linear fit yields the isotope shift (IS) of the ionization energy,

$$\mathrm{IS}[E_I(^6\mathrm{Li}\text{-}^7\mathrm{Li})] = -\,18\,067.54(21)\ \mathrm{MHz}. \tag{7}$$

The portion of this not related to nuclear charge distribution can be calculated from coefficients given in [7] as

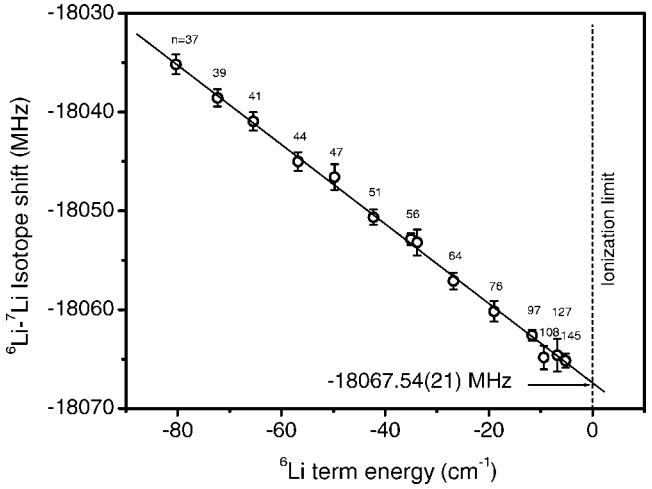

FIG. 7. ^{6}Li-^{7}Li isotope shifts in $n\,^2P$ Rydberg levels, referenced to respective ground level hfs c.g.'s, as a function of ^{6}Li term energy. The intercept is taken as the isotope shift of the ionization energy.

18 066.292(13) MHz; the residual difference of −1.25(21) MHz is then attributed to the nuclear field shift. This, in turn, can be related to the change in nuclear charge radii between two isotopes according to

$$\delta\langle r^2\rangle = \delta E_{\mathrm{nuc}}/C_{r^2}^{(0)}, \tag{8}$$

where the expansion coefficient $C_{r^2}^{(0)}$ is also given in [7], and higher-order terms are neglected as insignificant. This yields

$$\delta\langle r^2\rangle^{6-7} = 0.60(10)\ \mathrm{fm}^2, \tag{9}$$

which compares favorably with the value of 0.79(25) fm^2 determined by electron-nuclear scattering [41], as well as values of 0.61(11) fm^2 [4], 0.62(4) fm^2 [5], and 0.74(1) fm^2 [42] determined from Doppler-free optical measurements on the 2*S*-3*S* transition. The latter two values are derived from the same set of experimental data, but calculation of the mass-based shift in Ref. [42] finds substantially smaller relativistic recoil shifts than those from Ref. [7], which were used for $\delta\langle r^2\rangle$ derivation in Refs. [4,5]. The smaller recoil shift in Ref. [42] results from accidental cancellation among the reduced mass, mass polarization, and the direct electron-nucleus Breit interaction; and illustrates the need for continued improvement in these high-precision calculations. Other values ranging from 0.40 to 0.96 fm^2 have been derived from studies on one-photon transitions in Li^+ and Li, as reviewed in Ref. [43], but these are probably less reliable than the 2*S*-3*S* transition because of possible differential residual Doppler shifts, only partially resolved hyperfine structure, and the use of interferometric rather than frequency-based methods for determining the optical shifts. Further, only the 2*S*-3*S* transition has been used to study the radioactive isotopes ^{8,9,11}Li [4,5].

IV. CONCLUSIONS

While the current work has reduced the uncertainty in $E_I(^7\mathrm{Li})$ by about two orders of magnitude, and to a level comparable to the theoretical uncertainty, dramatic improvements are still possible. The major source of uncertainty in the current measurements is the energy of the reference 76 ^2P level. This could be significantly improved using femtosecond frequency metrology (FFM) [44] for determination of transition energies defining the reference level energy, which would reduce the wavemeter uncertainty to negligible levels. Such a remeasurement of the 76 ^2P level energy, combined with the current convergence analysis, could reduce overall uncertainty to the 3×10^{-5} cm^{-1} level. Repeating the full set of measurements with FFM would remove the interferometer scale uncertainty, and it is likely that the convergence limit would also be improved. The major remaining source of uncertainty would be from atomic beam–laser beam perpendicularity, which could be addressed by reexamining Doppler-free two-photon excitation of the $ns\,^2S$ and $nd\,^2D$ Rydberg series. While this failed with pulsed lasers because of molecular Li_2 interference at the relatively high temperatures and vapor densities in the heat pipe used, it is unlikely to be a problem with a weak atomic beam, high resolution lasers (which can resolve atomic lines from molecular), and mass spectrometric detection. Further, excitation with the standing wave inside a resonant enhancement cavity, as has been demonstrated for the 2*S*-3*S* transition [4,5], removes retrobeam pointing error. Resonant intensity enhancement also increases the two-photon excitation $\propto I^2$, and if a third photon is used for direct photoionization, the overall efficiency improves $\propto I^3$.

ACKNOWLEDGMENTS

Measurements reported in this work were performed at Pacific Northwest National Laboratory (PNNL) with support from the U.S. Department of Energy's Office of Science, Division of Chemical Sciences, Geosciences, and Biosciences. PNNL is operated for the US DOE by Battelle Memorial Institute. One of the authors (W.N.) acknowledges support from the Helmholtz Association under Contract No. VH-NG-148 and from BMBF under Contract No. 06TU203. The authors thank K. Pachucki for valuable discussions about residual differences between experiment and theory.

[1] Z.-C. Yan and G. W. F. Drake, Phys. Rev. Lett. **81**, 774 (1998).
[2] Z.-C. Yan, M. Tambasco, and G. W. F. Drake, Phys. Rev. A **57**, 1652 (1998).
[3] F. W. King, J. Mol. Struct.: THEOCHEM **400**, 7 (1997).
[4] G. Ewald, W. Nörtershäuser, A. Dax, S. Götte, R. Kirchner, H.-J. Kluge, T. Kühl, R. Sanchez, A. Wojtaszek, B. A. Bushaw *et al.*, Phys. Rev. Lett. **93**, 113002 (2004).
[5] R. Sanchez, W. Nörtershäuser, G. Ewald, D. Albers, J. Behr, P.

Bricault, B. A. Bushaw, A. Dax, J. Dilling, M. Dombsky *et al.*, Phys. Rev. Lett. **96**, 033002 (2006).
[6] A. S. Jensen, K. Riisager, D. V. Fedorov, and E. Garrido, Rev. Mod. Phys. **76**, 215 (2004).
[7] Z.-C. Yan and G. W. F. Drake, Phys. Rev. Lett. **91**, 113004 (2003).
[8] B. A. Bushaw, W. Nörtershäuser, G. Ewald, A. Dax, and G. W. F. Drake, Phys. Rev. Lett. **91**, 043004 (2003).
[9] L. J. Radziemski, R. Engleman, and J. W. Brault, Phys. Rev. A **52**, 4462 (1995).
[10] G. Ewald, Doctoral thesis, Ruprecht-Karls-Universität Heidelberg, 2005.
[11] C. E. Moore, *Ionization Potentials and Ionization Limits Derived from the Analysis of Optical Spectra* (U.S. Natl. Bur. Stand., Washington, DC, 1970), Vol. NSRDS-NBS 34.
[12] K. W. Meisner, L. G. Mundie, and P. H. Stelson, Phys. Rev. **74**, 932 (1948); **75**, 891 (1949).
[13] I. Johannson, Ark. Fys. **15**, 169 (1959).
[14] C.-J. Lorenzen and K. Niemax, Phys. Scr. **27**, 300 (1983).
[15] M. A. Baig, M. Akram, S. A. Bhatti, and N. Ahmad, J. Phys. B **27**, L351 (1994).
[16] M. Anwar-ul Haq, S. Mahmood, M. Riaz, R. Ali, and M. A. Baig, J. Phys. B **38**, S77 (2005).
[17] M. Ciocca, C. E. Burkhardt, J. J. Leventhal, and T. Bergeman, Phys. Rev. A **45**, 4720 (1992).
[18] S. A. Lee, J. Helmcke, J. A. Hall, and B. P. Stoicheff, Opt. Lett. **3**, 141 (1978).
[19] K.-H. Weber and C. J. Sansonetti, Phys. Rev. A **35**, 4650 (1987).
[20] E. Arnold, W. Bochers, B. Carré, H. T. Duong, P. Juncar, J. Lermé, S. Liberman, W. Neu, R. Neugart, E. W. Otten *et al.*, J. Phys. B **22**, L391 (1989).
[21] M. E. Koch and C. B. Collins, Phys. Rev. A **19**, 1098 (1979).
[22] C.-J. Lorenzen and K. Niemax, J. Phys. B **15**, L139 (1982).
[23] B. A. Bushaw, K. Blaum, and W. Nörtershäuser, Phys. Rev. A **67**, 022508 (2003).
[24] A. Schmitt, B. A. Bushaw, and K. Wendt, J. Phys. B **37**, 1633 (2004).
[25] R. Hergenröder, D. Veza, and K. Niemax, Spectrochim. Acta, Part B **48**, 589 (1993).
[26] G. D. Stevens, C.-H. Iu, S. Williams, T. Bergeman, and H. Metcalf, Phys. Rev. A **51**, 2866 (1995).
[27] W. Z. Zhao, J. E. Simsarian, L. A. Orozco, and G. D. Sprouse, Rev. Sci. Instrum. **69**, 3737 (1998).
[28] C. J. Sansonetti, B. Richou, R. Engleman, Jr., and L. J. Radziemski, Phys. Rev. A **52**, 2682 (1995).
[29] T. Udem, S. A. Diddams, K. R. Vogel, C. W. Oates, E. A. Curtis, W. D. Lee, W. M. Itano, R. E. Drullinger, J. C. Bergquist, and L. Hollberg, Phys. Rev. Lett. **86**, 4996 (2001).
[30] J. Stenger, T. Binnewies, G. Wilpers, F. Riehle, H. R. Telle, J. K. Ranka, R. S. Windeler, and A. J. Stentz, Phys. Rev. A **63**, 021802(R) (2001).
[31] D. J. Jones, S. A. Diddams, R. J. K, A. Stentz, R. S. Windeler, J. L. Hall, and S. T. Cundiff, Science **288**, 635 (2000).
[32] T. Udem, J. Reichert, T. W. Hänsch, and M. Kourogi, Phys. Rev. A **62**, 031801(R) (2000).
[33] M. L. Zimmerman, M. G. Littman, M. M. Kash, and D. Kleppner, Phys. Rev. A **20**, 2251 (1979).
[34] H. Rinneberg, J. Neukammer, G. Jönsson, H. Hieronymus, A. König, and K. Vietzke, Phys. Rev. Lett. **55**, 382 (1985).
[35] P. J. Mohr and B. N. Taylor, Rev. Mod. Phys. **77**, 1 (2005).
[36] G. Audi, A. H. Wapstra, and C. Thibault, Nucl. Phys. A **729**, 337 (2003).
[37] S. Nagy, T. Fritioff, M. Suhonen, R. Schuch, K. Blaum, M. Björkhage, and I. Bergström, Phys. Rev. Lett. **96**, 163004 (2006).
[38] P. Goy, J. Liang, M. Gross, and S. Haroche, Phys. Rev. A **34**, 2889 (1986).
[39] Z.-C. Yan and G. W. F. Drake, Phys. Rev. A **61**, 022504 (2000).
[40] W. DeGraffenreid and C. J. Sansonetti, Phys. Rev. A **67**, 012509 (2003).
[41] C. W. de Jager, H. de Vries, and C. de Vries, At. Data Nucl. Data Tables **14**, 479 (1974).
[42] M. Puchalski, A. M. Moro, and K. Pachucki, Phys. Rev. Lett. **97**, 133001 (2006).
[43] G. A. Noble, B. E. Schultz, H. Ming, and W. A. van Wijngaarden, Phys. Rev. A **74**, 012502 (2006).
[44] T. Udem, R. Holzwarth, and T. W. Hänsch, Nature (London) **416**, 233 (2002).